NCKU-HEP-00-03
IPAS-HEP-2003
APCTP-00-09
hep-ph/0006yyy

arXiv:hep-ph/0006001v1 1 Jun 2000

Nonleptonic charmless B decays: factorization vs perturbative QCD*

Yong-Yeon Keum[1] † **and Hsiang-nan Li**[2] ‡

[1] *Institute of Physics, Academia Sinica,*
Taipei, Taiwan 105, Republic of China

[2] *Department of Physics, National Cheng-Kung University,*
Tainan, Taiwan 701, Republic of China

We compare the factorization approach, the perturbative QCD approach and the Beneke-Buchalla-Neubert-Sachrajda approach to nonleptonic charmless B meson decays. We discuss their treatments of factorizable, nonfactorizable, and annihilation contributions, infrared-cutoff and scale dependences, and strong phases. It is proposed that measurement of CP asymmetries in two-body B meson decays provides an appropriate test of the these approaches.

PACS index : 13.25.Hw, 11.10.Hi, 12.38.Bx, 13.25.Ft

---

* Some parts of this paper were presented at the Sapporo Winter School 2000, March 3-7, 2000 in Japan

†Email: keum@phys.sinica.edu.tw
‡Email: hnli@mail.ncku.edu.tw

I. INTRODUCTION

Exclusive nonleptonic B meson decays provide information of important dynamics such as penguin contributions, CP asymmetries, and weak and strong phases. However, it is difficult to analyze these processes because of their nonperturbative origin. To simplify the analysis, the factorization approximation (FA) has been applied to decay amplitudes, under which nonfactorizable and annihilation contributions are neglected, and factorizable contributions are expressed as products of Wilson coefficients, meson decay constants, and hadronic transition form factors. In this paper we shall compare three approaches to nonleptonic charmless B meson decays, which are more or less related to FA: the FA approach [1], the perturbative QCD (PQCD) approach [2–4], and the Beneke-Buchalla-Neubert-Sachrajda (BBNS) approach [5,6]. We take the $B \to \pi\pi$ decays as an example, and explain how factorizable, nonfactorizable, and annihilation contributions, infrared-cutoff and scale dependences, and strong phases are treated in these approaches.

The effective Hamiltonian for the $B \to \pi\pi$ decays is given by [7]

$$H_{\rm eff} = \frac{G_F}{\sqrt{2}} \sum_{q=u,c} V_q \left[C_1(\mu) O_1^{(q)}(\mu) + C_2(\mu) O_2^{(q)}(\mu) + \sum_{i=3}^{10} C_i(\mu) O_i(\mu) \right] , \tag{1}$$

with the Cabibbo-Kobayashi-Maskawa (CKM) matrix elements $V_q = V_{qd}^* V_{qb}$ and the four-fermion operators

$$\begin{aligned}
&O_1^{(q)} = (\bar{d}_i q_j)_{V-A} (\bar{q}_j b_i)_{V-A} , \qquad O_2^{(q)} = (\bar{d}_i q_i)_{V-A} (\bar{q}_j b_j)_{V-A} , \\
&O_3 = (\bar{d}_i b_i)_{V-A} \sum_q (\bar{q}_j q_j)_{V-A} , \quad O_4 = (\bar{d}_i b_j)_{V-A} \sum_q (\bar{q}_j q_i)_{V-A} , \\
&O_5 = (\bar{d}_i b_i)_{V-A} \sum_q (\bar{q}_j q_j)_{V+A} , \quad O_6 = (\bar{d}_i b_j)_{V-A} \sum_q (\bar{q}_j q_i)_{V+A} , \\
&O_7 = \frac{3}{2} (\bar{d}_i b_i)_{V-A} \sum_q e_q (\bar{q}_j q_j)_{V+A} , \quad O_8 = \frac{3}{2} (\bar{d}_i b_j)_{V-A} \sum_q e_q (\bar{q}_j q_i)_{V+A} , \\
&O_9 = \frac{3}{2} (\bar{d}_i b_i)_{V-A} \sum_q e_q (\bar{q}_j q_j)_{V-A} , \quad O_{10} = \frac{3}{2} (\bar{d}_i b_j)_{V-A} \sum_q e_q (\bar{q}_j q_i)_{V-A} ,
\end{aligned} \tag{2}$$

where i, j are color indices and μ a renormalization scale.

Decay amplitudes are written as

$$\begin{aligned}
\mathcal{M} &\propto \langle \pi(P_2)\pi(P_3)|H_{\rm eff}|B(P_1)\rangle , \\
&\propto \sum_i C_i(\mu) \langle \pi(P_2)\pi(P_3)|O_i(\mu)|B(P_1)\rangle ,
\end{aligned} \tag{3}$$

with the meson momenta P_i. For convenience, we assume $P_1 = (P_1^+, P_1^-, \mathbf{P}_{1T}) = (M_B/\sqrt{2})(1, 1, 0_T)$, $P_2 = (M_B/\sqrt{2})(1, 0, 0_T)$, and $P_3 = (M_B/\sqrt{2})(0, 1, 0_T)$, M_B being the B meson mass. The dependences on the renormalization scale μ cancel between the Wilson coefficients $C_i(\mu)$ and the hadronic matrix elements $\langle \pi\pi|O_i(\mu)|B\rangle$, such that the decay amplitudes are scale-independent (and also scheme-independent). In the practical derivation of the effective Hamiltonian, an infrared cutoff for loop integrals needs to be introduced, since four-fermion amplitudes may contain soft divergences, which are related to nonperturbative dynamics involved in the matrix elements. If the infrared cutoff appears in the form that external fermions are off-shell,

the derivation will even become gauge dependent [8]. These potential infrared-cutoff and gauge dependences are usually hidden in the matrix elements.

In the FA approach the matrix element of, say, O_2 is expressed as

$$\begin{aligned}\langle\pi(P_2)\pi(P_3)|O_2(\mu)|B(P_1)\rangle &\approx \langle\pi(P_2)|(\bar{d}_i q_i)_{V-A}|0\rangle\langle\pi(P_3)|(\bar{q}_j b_j)_{V-A}|B(P_1)\rangle\ ,\\ &\propto f_\pi F^{B\pi}(q^2=M_\pi^2)\ ,\end{aligned} \tag{4}$$

where f_π is the pion decay constant and $F^{B\pi}(M_\pi^2)$ the $B\to\pi$ transition form factor evaluated at $q^2=M_\pi^2$, M_π being the pion mass. The form factor itself is parametrized by models. Though analyses are simple under FA, a serious problem arises. When decay amplitudes are expressed as the products of μ-dependent Wilson coeficients and μ-independent hadronic form factors, they depend on the scale μ. A cure of this scale dependence has been proposed in [9,10], which will be discussed in Sec. II.

The PQCD approach to exclusive B meson decays has been developed some time ago [11,12]. PQCD is a method to separate hard components from a QCD process, which are treated by perturbation theory. Nonperturbative components are organized in the form of hadron wave functions, which can be extracted from experimental data. This formalism, so-called factorization theorem, has been successfully applied to various semileptonic decays [11,12] and nonleptonic (charmed and charmless) decays [2,3,13–16]. For the $B\to\pi\pi$ decays, the hard amplitude involves six external on-shell quarks, four of which correspond to the four-fermion operators and two of which are the spectator quarks in the B and π mesons. Since nonperturbative dynamics has been factored out, one can evaluate all possible Feynman diagrams for the six-quark amplitude straightforwardly, which include both factorizable and nonfactorizable contributions. Factorizable and nonfactorizable annihilation diagrams are also included. That is, FA is not necessary in the PQCD approach. Without FA, the scale independence can be achieved easily [17]. It has been shown that nonperturbative meson wave functions, being universal, are the same for various topologies of diagrams in all decay modes, which contain the B and π mesons.

Recently, Beneke *et al.* proposed an alternative formalism for two-body charmless B meson decays [5]. They claimed that factorizable contributions (the form factor $F^{B\pi}$ in this case) are not calculable in PQCD, but nonfactorzable contributions are in the heavy quark limit. Hence, the former are treated in the same way as in the FA approach, and expressed as products of Wilson coefficients and $F^{B\pi}$. The latter, calculated as in the PQCD approach, are written as the convolutions of hard amplitudes with three (B,π,π) meson wave functions. Annihilation diagrams are neglected as in FA. Therefore, this formalism can be regarded as a mixture of the FA and PQCD approaches. Values of form factors at maximal recoil $q^2=M_\pi^2$ and nonperturbative meson wave functions are all treated as free parameters. The BBNS approach then involves more parameters compared to FA and PQCD. This approach has been applied to the $B\to\pi\pi$ and $K\pi$ decays [6].

In this work we shall make a detailed comparision of the above three approaches to nonleponic charmless B meson decays. We discuss their treatments of the infrared-cutoff and scale dependences in Sec. II, factorizable contributions in Sec. III, nonfactorizable contributions in Sec. IV, and annihilation contributions and strong phases in Sec. V. It will be shown that the CP asymmetry of the $B_d^0\to\pi^\pm\pi^\mp$ decays predicted in PQCD is

much larger than in the FA and BBNS approaches. Hence, the measurement of CP asymmetries will provide an appropriate test of these predictions. Section VI is the summary. Note that final-state-interaction (FSI) effects are always assumed to be absent in the above three approaches. The neglect of FSI effects has been argued in [4].

II. SCALE DEPENDENCE

As stated in the Introduction, a serious problem of FA is the dependence of physical predictions on the renormalization scale μ. A plausible solution to the aforementioned problem has been proposed in [9,10]. The idea is to extract a μ-dependent evolution factor $g(\mu)$ from the matrix element $\langle\pi\pi|O(\mu)|B\rangle$, and combine it with the μ-dependent Wilson coefficient $C(\mu)$:

$$\mathcal{M} \propto C(\mu)\langle\pi\pi|O(\mu)|B\rangle = C(\mu)g(\mu)\langle\pi\pi|O|B\rangle_{\rm tree} \equiv C^{\rm eff}\langle\pi\pi|O|B\rangle_{\rm tree} \ , \tag{5}$$

where the effective Wilson coefficient $C^{\rm eff}$ is μ-independent. The extraction of $g(\mu)$ involves the mixing of effective operators below the scale μ and above the lower scale m_b, m_b being the b quark mass. After making a physical amplitude explicitly scale-independent, FA is applied to the matrix element at the tree level,

$$\langle\pi\pi|O|B\rangle_{\rm tree} \propto f_\pi F^{B\pi} \ . \tag{6}$$

This strategy has also been adopted in the BBNS approach.

The above issue is in fact much subtler. One-loop corrections to on-shell b quark decay amplitudes are usually infrared divergent [8]. To remove these infrared divergences, the conventional treatment is to assume that external quarks are off-shell by $-p^2$. This assumption, however, results in a gauge dependence of one-loop corrections. The evolution factor $g(\mu)$ then depends on an infrared cutoff $-p^2$ and on a gauge parameter, which are originally implicit in the matrix element. Therefore, the modified FA, though removes the scale dependence of a decay amplitude, often introduces the infrared-cutoff and gauge dependences.

The controversy of the scale, infrared-cutoff and gauge dependences can be resolved in the PQCD approach [17]. In this formalism partons, *i.e.*, external quarks, are assumed to be on shell, and both ultraviolet and infrared divergences in radiative corrections are isolated using the dimensional regularization. With external quarks being on shell, gauge invariance of a decay amplitude is guaranteed under radiative corrections. The ultraviolet poles are subtracted in a renormalization scheme. The infrared poles, which correspond to nonperturbative dynamics of decay processes, are absorbed into meson wave functions. How much finite piece of radiative corrections is absorbed into wave functions along with the infrared poles depends on a factorization scheme, or equivalently, on a factorization scale μ_f. In the PQCD approach μ_f has been chosen as the inverse of the meson transverse extent, $1/b$. In other words, dynamics below (above) the factorization scale is absorbed into a nonperturbative wave function (perturbative hard amplitude), and a decay amplitude is factorized into convolution of these two subprocesses.

For nonleptonic B meson decays, contributions above the factorization scale involve two scales: M_W, at which the matching conditions of the effective weak Hamiltonian to the full Hamiltonian are defined, and the typical

scale t of a hard amplitude, which reflects specific dynamics of a decay mode. The scale t, corresponding to the lower scale m_b in the modified FA, is chosen as the maximal virtuality of internal particles in a hard amplitude. The analysis of next-to-leading-order corrections to the pion form factor [18] has indicated that this choice minimizes higher-order corrections.

Without assuming FA, the μ dependence of a decay amplitude is calculated based on six-fermion hard amplitudes in the PQCD approach. Radiative corrections produce various types of logarithms: $\ln(M_W/\mu)$, $\ln(\mu/t)$ and $\ln(tb)$. The renormalization-group (RG) summation of the first type of logarithms leads to the Wilson coefficients $C(\mu)$ in Eq. (5). The second and third types are summed into the evolution factor

$$g(\mu) \equiv g_1(\mu, t) g_2(t, 1/b) \; . \tag{7}$$

The above expression implies that g in fact contains two pieces, g_1 and g_2, which are governed by different anomalous dimensions. The anomalous dimension of g_1 is the same as of $C(\mu)$. Below the hard scale t, loop corrections associated with spectator quarks contribute, such that the anomalous dimension of g_2 differs from that of g_1 [17].

Insert Eq. (7) into Eq. (5), the effective Wilson coefficient is written as

$$C^{\rm eff} \equiv C(t) g_2(t, 1/b) \; , \tag{8}$$

which consists of two stages of RG evolutions. We have extended the Wilson evolution directly from M_W down to t without further considering the mixing of effective operators. The scale independence of a decay amplitude is thus constructed explicitly. The Wilson evolution is then followed by the second-stage evolution from t down to $1/b$, which plays the role of the infrared cutoff $-p^2$.

Together with the second-stage RG evolution, there also exists the Sudakov evolution $\exp[-s(P,b)]$ from the resummation of double logarithms $\ln^2(Pb)$ [19,20], which arise from the overlap of collinear and soft divergences in radiative corrections to meson wave functions, P denoting the dominant light-cone component of meson momentum. The effect of the Sudakov evolution will be explained in the next section. After summing all various large logarithms, the hard amplitude $H(t)$ can be evaluated at the characteristic scale t perturbatively. $H(t)$ contains all possible factorizable and nonfactorizable diagrams.

At last, we address the treatment of the dependence on the factorization scale in the PQCD approach. Both the hard amplitudes and the meson wave functions $\phi(x,b)$, x being the momentum fraction associated with a valence quark, depend on factorization schemes. For example, $\phi(x,b)$ and $\phi(x,b/2)$ are different. However, a decay amplitude, as convolution of the two subprocesses, does not depend on factorization schemes. The wave functions, though not calculable, are universal (process-independent), since they absorb long-distance dynamics, which is insensitive to the specific decay of the b quark into light quarks with large energy release. In the practical application $\phi(x,b/c)$ for the factorization scale c/b, c being a constant of order unity, can be determined from experimental data of some decay modes. These wave functions are then employed to make predictions for other modes, whose factorizations are constructed at the same scale c/b. With this prescription, the dependence on the factorization scale is removed. Usually, c is chosen as unity.

A three-scale factorization formula for exclusive nonleptonic B meson decays is then written as

$$C(t) \otimes H(t) \otimes \phi(x,b) \otimes g_2(t,b) \otimes \exp\left[-s(P,b)\right] \ . \tag{9}$$

Note that Eq. (9) is a convolution relation, with internal parton kinematic variables x and b integrated out (t depends on x and b as defined later). All the convolution factors, except for the wave functions $\phi(x,b)$, are calculable in perturbation theory. Comparing Eq. (9) with Eq. (5), the tree-level matrix element is read off as

$$\langle \pi\pi|O|B\rangle_{\rm tree} = H(t) \otimes \phi(x,b) \otimes \exp\left[-s(P,b)\right] \ . \tag{10}$$

If choosing t as m_b, Eq. (9) reduces to a simple product of the constant Wilson coefficient $C(m_b)$ and the hadronic matrix element.

III. FACTORIZABLE CONTRIBUTIONS

In the FA approach factorizable contributions are expressed as products of Wilson coefficients and transition form factors, which are then parametrized by some models. This treatment of factorizable contributions has also been adopted in the BBNS approach. It has been argued that the $B \to \pi$ transition form factor $F^{B\pi}$ can not be evaluated in PQCD, because the on-shellness of internal particles in the hard amplitude is not suppressed by meson wave functions [5]. For example, the lowest-order hard amplitude in Fig. 1 consists of the internal b quark and gluon propagators proportional to

$$\frac{1}{[(P_1-k_3)^2-m_b^2](k_1-k_3)^2} = \frac{1}{(2P_1\cdot k_3)(2k_1\cdot k_3)} = \frac{1}{x_1 x_3^2 M_B^4} \ , \tag{11}$$

where k_1 (k_3) is the momentum of the spectator quark in the B (π) meson, and $x_1 = k_1^+/P_1^+$ ($x_3 = k_3^-/P_3^-$) the corresponding momentum fraction as indicated in Fig. 1. To derive the above expression, we have neglected the mass difference $\bar{\Lambda} = M_B - m_b$. Obviously, the pion wave function, if proportional to $x_3(1-x_3)$, does not remove the power divergence at $x_3 \to 0$ from the on-shell internal particles. The assumption that internal particles in a hard amplitude should be off-shell is then violated, and PQCD is not applicable to $F^{B\pi}$.

A different viewpoint has been adopted in the PQCD approach. Since the end-point divergence is not of the pinched type, which is absorbed into a wave function, we argue that it can be either killed by a pion wave function vanishing faster than x_3 as $x_3 \to 0$, or smeared out by parton transverse momenta k_T [21]. Including k_T, Eq. (11) becomes

$$\frac{1}{(x_3 M_B^2 + k_{3T}^2)[x_1 x_3 M_B^2 + (\mathbf{k}_{1T} - \mathbf{k}_{3T})^2]} \ , \tag{12}$$

which has no singularity at $x_3 \to 0$. As argued in [21], partons can carry small amount of transverse momenta. When the end-point region with $x \to 0$ is not important, it is proper to approximate Eq. (12) for the hard amplitude by Eq. (11), and the transverse degrees of freedom of partons in meson wave functions can be integrated out. When the end-point region is important as in the case of $F^{B\pi}$, one should keep k_T for a consistent analysis. Once the transverse degrees of freedom of partons are taken into account, the factorization

of a QCD process should be performed in the b space, b being the variable conjugate to k_T [20]. This is how the factorization scale $1/b$ is introduced in the previous seciton.

As stated before, the scale t should be chosen as the maximal virtuality of internal particles in a hard amplitude,

$$t = \max(\sqrt{x_1 x_3} M_B, \sqrt{x_3} M_B, 1/b) \; , \tag{13}$$

according to Eq. (12). The Sudakov factor $\exp[-s(P,b)]$ suppresses the long-distance contributions in the large b region, and vanishes as $b = 1/\Lambda_{\rm QCD}$, $\Lambda_{\rm QCD}$ being the QCD scale. This factor then guarantees that most contributions to decay amplitudes come from the region with small coupling constant $\alpha_s(t)$ [21]. It has been shown that 97% of the contribution to $F^{B\pi}$ arises from the region with $\alpha_s(t)/\pi < 0.3$ [4]. It indicates that $F^{B\pi}$ at large recoil of the pion is well within the perturbative regime, and that dynamics from hard gluon exchanges dominates. This is the reason PQCD with Sudakov suppression is applicable to exclusive decays around the energy scale of the B meson mass [12]. The above conclusion is consistent with the following physical picture. The $B \to \pi$ transition occurs via the $b \to u$ decay with the outgoing u quark being energetic. The spectator quark of the B meson is more or less at rest. The probability that this spectator quark and the u quark with large relative velocity form the pion is strongly suppressed by the pion wave function and by the Sudakov factor. Therefore, the process dominates, where a hard gluon is exchanged so that the two quarks are aligned to form the pion.

We need to illuminate another concept about the application of PQCD. The smallness of PQCD predictions compared to experimental data does not definitely imply that perturbative contribution is not important [22]. PQCD predictions depend on wave funcitons one adopts. For example, a smooth B meson wave function decreases PQCD predictions for $F^{B\pi}$ by a huge extent. However, this smooth B meson wave function may not be correct, such that a conclusion drawn from it is not valid. In our analysis the B meson and pion wave functions are determined from the data of the pion form factor and of the $B \to D\pi(\rho)$ decays. We then employ the extracted wave funcitons to predict $F^{B\pi}$ and examine the dominance of perturbative contributions. In this way the ambiguity in choosing wave functions and the model dependence of PQCD predictions are reduced.

Below we highlight the enhancement of penguin contributions observed in the PQCD approach, and its role in the explanation of the $B \to \pi\pi$ and $B \to K\pi$ data. For simplicity, we present the observation by means of the FA approach. Consider the ratios R and R_π,

$$R = \frac{{\rm Br}(B^0 \to K^\pm \pi^\mp)}{{\rm Br}(B^\pm \to K^0 \pi^\mp)} = \frac{a_K^2 + 2 a_K \lambda^2 R_b \cos\phi_3}{a_K^2} \; , \tag{14}$$

$$R_\pi = \frac{{\rm Br}(B^0 \to K^\pm \pi^\mp)}{{\rm Br}(B^0 \to \pi^\pm \pi^\mp)} = \frac{a_K^2 + 2 a_K \lambda^2 R_b \cos\phi_3}{\lambda^2 R_b [R_b + 2 a_\pi (R_b - \cos\phi_3)]} \; , \tag{15}$$

with the Wolfenstein parameters λ and R_b, and the Wilson coefficients

$$a_1 = C_2 + \frac{C_1}{N_c} \; ,$$
$$a_4 = C_4 + \frac{C_3}{N_c} + \frac{3}{2} e_q \left(C_{10} + \frac{C_9}{N_c} \right) \; ,$$

$$a_6 = C_6 + \frac{C_5}{N_c} + \frac{3}{2} e_q \left(C_8 + \frac{C_7}{N_c} \right) , \tag{16}$$

N_c being the number of colors. The factor

$$a_{K(\pi)} = \frac{a_4 + 2 r_{K(\pi)} a_6}{a_1} , \quad r_{K(\pi)} = \frac{M^2_{K(\pi)}}{M_B (m_{s(u)} + m_d)} , \tag{17}$$

being negative, represents the ratio of the penguin contribution to the tree contribution in the $K\pi(\pi\pi)$ mode, where $M_{K(\pi)}$ is the kaon (pion) mass and m_q, $q = s$, u, and d, the q quark masses.

It is obvious that the data $R \sim 1$ [23] imply the unitarity angle $\phi_3 \sim 90^o$, no matter what a_K, λ and R_b are. Therefore, R is an appropriate quantity for the determination of ϕ_3. While to determine ϕ_3 from the data of the ratio $R_\pi \sim 4$ [23], one must have precise information of a_K, a_π, λ and R_b. It can be shown that the extraction of ϕ_3 from R_π depends on these parameters sensitively. Hence, R_π is not an appropriate quantity for the determination of ϕ_3. To explain $R_\pi \sim 4$, a large $|a_\pi| \sim 0.1$ corresponding to $m_d = 2m_u = 3$ MeV and a large $\phi_3 \sim 130^o$ must be adopted in the FA approach [24]. This is obvious from Eq. (15), since a large ϕ_3 leads to a constructive interference between the first and second terms in the numerator of R_π. In the modified FA approach with effective number of colors $N_c^{\rm eff}$, a large unitarity angle $\phi_3 \sim 105^o$ is also concluded [25].

It is interesting to ask whether one can explain $R_\pi \sim 4$ using reasonable quark masses $m_d = 2m_u \sim 10$ MeV and a smaller $\phi_3 \sim 90^o$, if the extraction from R is given a higher weight. The answer is positive in the PQCD approach. An essential difference between the FA and BBNS approaches and the PQCD approach is that transition form factors can be calculated in the latter as argued above. Therefore, we do not assume that the form factors associated with the Wilson coefficients $a_{1,4}$ and with a_6 are the same. An explicit PQCD calculation indicates that the ratios $a_{K,\pi}$ are more complicate, which reduce to Eq. (17) only in some extreme kinematic conditions of partons [4]. Moreover, the choice of the hard scale t, at which Wilson coefficients are evaluated, is also different. It is chosen arbitrarily as m_b or $m_b/2$ in the FA and BBNS approaches, but as virtuality of internal particles of a hard amplitude in PQCD, such that evolution effects vary among the above form factors.

It has been noticed that $a_1(\mu)$, $a_4(\mu)$ and $a_6(\mu)$ have dramatically different μ dependences for $\mu < m_b/2$: $|a_4|$ and $|a_6|$ increase with the decrease of μ faster than a_1. The choice of the scale in PQCD makes possible that t runs to below $m_b/2$, and that penguin contributions are enhanced over tree contributions. It has been observed that the evolution effect enhances the ratios $|a_{K,\pi}|$ by about 50% [4]. Hence, even adopting $m_d = 2m_u \sim 10$ MeV, we can account for $R_\pi \sim 4$ using $\phi_3 \sim 90^o$. That is, the data of R_π do not demand large ϕ_3. We emphasize that the hard scale t with an average 1.4 GeV, corresponding to $\alpha_s(t)/\pi \sim 0.13$, is still large enough to guarantee the applicability of PQCD [4].

IV. NONFACTORIZABLE CONTRIBUTIONS

Nonfactorizable contributions are neglected in the FA approach. However, it has been known that this approximation is not always appropriate, especially for the decay modes, whose factorizable amplitudes are

proportional to the Wilson coefficient $a_2 = C_1 + C_2/N_c$. Since a_2 is small, factorizable contributions and nonfactorizable contributions are of the same order, and the latter become important. This is the reason it is difficult to resolve the controversy in the branching ratios of the $B \to J/\psi K^{(*)}$ decays in FA [3]. The conventional way to introduce nonfactorizable contributions is to vary number of colors in the Wilson coeficients a_i. The resultant effective number of colors, $N_c^{\rm eff}$, being process-dependent parameters, render the FA approach less predictive.

To go beyond FA, it has been proposed to evaluate nonfactorizable amplitudes for two-body charmless B meson decays using PQCD factorization theorem in the BBNS approach [5]. The motivation is that the power divergence appearing in $F^{B\pi}$ does not exist in nonfactorizable amplitudes, since soft divergences cancel between the two diagrams in Fig. 2 [5]. Hence, these diagrams contribute to the hard parts of the $B \to \pi\pi$ decays, and are calculable in PQCD. We emphasize that the above soft cancellation is not sufficient to justify the applicability of PQCD. No matter what value M_B is, one can always obtain the soft cancellation between the two nonfactorizable diagrams. However, it is obvious that PQCD is not applicable to B meson decays if M_B is as low as 1 GeV. The criterion for the applicability of PQCD is stronger: PQCD is applicable only when higher-order corrections to decay amplitudes are under control.

We shall show explicitly, following the reasoning in [26], that the simple factorization formula in [5] for a nonfactorizable amplitude suffers large higher-order corrections. The expression is

$$f = C\alpha_s \int \frac{dx_1}{x_1}\phi_B(x_1)\left[\int \frac{dx}{x}\phi_\pi(x)\right]^2 , \tag{18}$$

where the constant C is related to a color factor, the denominator $x_1 x$ comes from the hard gluon propagator, and another denominator x comes from the internal quark propagator. If the hard part is characterized by M_B, the coupling constant α_s evaluated at the scale $\mu \sim M_B$ is small and higher-order corrections are negligible. However, it is not the case. When including higher-order corrections that cause the running of α_s, the logarithm $\alpha_s(\mu)\ln(x_1 x M_B^2/\mu^2)$ occurs, with $x_1 x M_B^2$ being the invariant mass of the hard gluon. In order to diminish this logarithmic correction, the appropriate choice of the scale is $\mu = \sqrt{x_1 x}M_B$. The coupling constant α_s in Eq. (18) becomes running and should move into the convolution relation, leading to

$$f = C \int \frac{dx_1}{x_1}\phi_B(x_1)\frac{dx_2}{x_2}\phi_\pi(x_2)\frac{dx_3}{x_3}\phi_\pi(x_3)\alpha_s(\sqrt{x_1 x_3}M_B) . \tag{19}$$

Assume the following models for the meson wave functions:

$$\phi_B(x) = N_B\sqrt{x(1-x)}\exp\left(-\frac{M_B^2 x^2}{2\omega_B^2}\right) , \tag{20}$$

$$\phi_B'(x) = N_B' x^2(1-x)^2\exp\left(-\frac{M_B^2 x^2}{2\omega_B'^2}\right) , \tag{21}$$

$$\phi_\pi(x) = \frac{\sqrt{6}}{2}f_\pi x(1-x) . \tag{22}$$

The B meson wave functions ϕ_B [27] and ϕ_B' [4] possess peaks at small x that depend on the shape parameters ω_B and ω_B', respectively. According to [5], the values of the shape parameters can be fixed via the parameter $\lambda_B = 0.3$ GeV:

$$\frac{\int_0^1 (dx/x)\phi_B(x)}{\int_0^1 dx\phi_B(x)} = \frac{M_B}{\lambda_B} = 17.6\ , \tag{23}$$

which gives $\omega_B = 0.65$ GeV and $\omega'_B = 0.25$ GeV. The normalization constant N_B is related to the B meson decay constant f_B through $\int_0^1 \phi_B(x)dx = f_B/(2\sqrt{2N_c})$. The asymptotic pion wave function in Eq. (22) has been adopted in [5].

Using the wave function $\phi_B(\phi'_B)$, we find that only about 20% (30%) of the full contribution to the nonfactorizable amplitude comes from the perturbative region with $\alpha_s/\pi < 0.3$. To derive the above percentages, we have chosen $\Lambda_{\rm QCD} = 250$ MeV for the running α_s, and frozen the scale $\sqrt{x_1 x_3}M_B$ to 0.4 GeV, as it goes to below 0.4 GeV. We conclude that Eq. (19) is dominated by soft contribution from the end-point region with $x_1, x \to 0$, *i.e.*, with $\alpha_s > 1$, where the perturbative expansion is not justified. Therefore, nonfactorizable contributions can not be evaluated reliably in the BBNS approach. This conclusion is consistent with that drawn in [26]: PQCD without Sudakov suppression is not applicable to exclusive processes for an energy scale below 10 GeV. The formalism in [5] is self-consistent as $M_B \to \infty$, but not in the case with $M_B \sim 5$ GeV.

In the end-point region where soft contributions are important, nonfactorizable amplitudes should be treated in a more careful way. That is, the dependence on the parton transverse momentum k_T is essential, and should be included as argued in the previous section. The argument of α_s is also set to t, the maximal virtuality of internal particles of a hard amplitude, which is similar to that in Eq. (19), but depends on the additional scale $1/b$. $\alpha_s(t)$ is then always small even in the end-point region, since $1/b$ is large under Sudakov suppression [21]. It has been shown that almost 100% of full contributions to nonfactorizable amplitudes arise from the region with $\alpha_s(t)/\pi < 0.3$. That is, the evaluation of nonfactorizable contributions is reliable in the PQCD approach.

There is another difference between the BBNS and PQCD approaches in the treatment of nonfactorizable contributions. The momentum of the light spectator quark in the B meson has been ignored in the former [5], such that quark propagators in the hard part always remain time-like:

$$\frac{1}{(k_2+k_3-k_1)^2+i\epsilon} \approx \frac{1}{(k_2+k_3)^2} = \frac{1}{x_2 x_3 M_B^2}\ . \tag{24}$$

This approximation drops the strong phase from the kinematic region where the virtual quark becomes on-shell, $(k_2+k_3-k_1)^2 \sim 0$. In the PQCD approach nonfactorizable contributions are complex:

$$\frac{1}{(k_2+k_3-k_1)^2+i\epsilon} = P\left[\frac{1}{(k_2+k_3-k_1)^2}\right] - i\pi\delta\left[(k_2+k_3-k_1)^2\right]\ , \tag{25}$$

where P denotes the principle-value prescription. As shown in [16], the above imaginary part is not the main source of strong phases for the $B \to \pi\pi$ decays, because nonfactorizable contributions are only few percents of factorizable ones. However, it will become important in decay modes whose factorizable amplitudes are proportional to the small Wilson coefficient a_2, or absent, such as the $B_d^0 \to K^\pm K^\mp$ decays [28].

V. STRONG PHASES

In the FA and BBNS approaches annihilation contributions have been neglected. Though annihilation amplitudes from the operator O_4 for the $B \to \pi\pi$ decays indeed vanish because of helicity suppression, those from

O_6 do not. As shown in Eqs. (B1) and (B6) of [29], there is a large enhancing factor

$$\frac{M_B^2}{(m_b+m_d)(m_u+m_d)} \ , \tag{26}$$

associated with annihilation contributions from O_6, which is much larger than the one

$$\frac{M_\pi^2}{(m_b+m_d)(m_u+m_d)} \ , \tag{27}$$

associated with usual penguin contributions. Though annihilation contributions are suppressed by a factor f_B/M_B [30], they can be comparible with penguin contributions. It has been observed that the annihilation diagrams Figs. 3(e) and 3(f) contribute large imaginary parts (strong phases) in the PQCD approach [4].

In the approaches where annihilation contributions are neglected, strong phases must be introduced via the Bander-Silverman-Soni (BSS) mechanism shown in Fig. 4(a) [31]. However, this mechanism, contributing through a charm quark loop, is suppressed by the charm mass threshold [4]:

$$q^2=(x_2P_2+x_3P_3)^2=x_2x_3M_B^2>4m_c^2 \ , \tag{28}$$

m_c being the c quark mass. Obviously, the large x_2 and x_3 regions are not favored by the pion wave funtion in Eq. (22). . Moreover, the diagram with a charm quark loop is of higher order in the PQCD formalism. An exact numerical analysis has indicated that the imaginary contribution from the BSS mechanism is smaller than that from the annihilation diagrams by a factor 10 [4].

Another source of strong phases in the FA and BBNS approaches is the diagrams in Fig. 4(b), whose imaginary contributions appear in the effective Wilson coefficients in Eqs.(4)-(8) of [5], for instance,

$$\begin{aligned} a_1^u &= C_1+\frac{C_2}{N}+\frac{\alpha_s}{4\pi}\frac{C_F}{N}C_2F \ , \\ F &= -12\ln\frac{\mu}{m_b}-18+f_\pi^I+f_\pi^{II} \ , \end{aligned} \tag{29}$$

with

$$f_\pi^I=-0.5-3\pi i \ , \tag{30}$$

and f_π^{II} being real. We emphasize that Eq. (30) is derived from a configuration, in which the outgoing $\bar{u}$ quark carries the full pion momentum. Again, this configuration is strongly suppressed by the pion wave function and by the Sudakov factor. That is, the imaginary contribution from the above source has been overestimated.

Below we make a quantative comparision among the FA, BBNS and PQCD approaches. Figure 3 collects all the Feynman diagrams for the hard amplitude of the $B_d^0\to\pi^+\pi^-$ decay, including factorizable and non-factorizable tree, penguin and annihilation diagrams, whose contributions are listed in Table I. The results obtained in the BBNS approach are also shown. The FA results are the same as the BBNS ones, but with the nonfactorizable amplitudes neglected. We observe

1. The tree contributions are almost equal in the three approaches, but the penguin contributions are larger in PQCD, corresponding to a larger ratio $|a_\pi|$ defined by Eq. (17) (about twice of those in FA and BBNS), *i.e.*, corresponding to the dynamical penguin enhancement.

2. The tree and penguin contributions are real in PQCD, but complex in FA and BBNS due to the complex effective Wilson coefficients, which are the main source of strong phases in FA and BBNS.

3. The annihilation contributions are neglected in FA and BBNS, but of the same order as the penguin contributions in PQCD, which are the main source of strong phases in PQCD.

4. Nonfactorizable contributions are complex in PQCD but real in BBNS, as explained in the previous section, and neglected in FA. Note that different B and π meson wave functions have been employed as deriving the results in Table I [4,5]. Nonfactorizable contributions are destructive relative to the penguin contributions, if concering only the real parts, and negligible for the $B \to \pi\pi$ branching ratios in both approaches.

5. The dominant nonfactorizable contribution M^P in BBNS is due to the sharp hard parts in the end-point regions of momentum fractions x as stated in Sec. III.

6. The total tree and penguin contributions, including both factorizable, nonfactorizable and annihilation ones, are

$$\begin{aligned} T_{\rm PQCD} &= (71.87 + 3.20i) \times 10^{-3} \,, \quad P_{\rm PQCD} = (-7.47 + 4.64i) \times 10^{-3} \,, \\ T_{\rm BBNS} &= (74.93 + 1.13i) \times 10^{-3} \,, \quad P_{\rm BBNS} = (1.13 - 1.27i) \times 10^{-3} \,, \\ T_{\rm FA} &= (75.70 + 1.13i) \times 10^{-3} \,, \quad P_{\rm FA} = (-3.04 - 1.27i) \times 10^{-3} \,. \end{aligned} \tag{31}$$

The tree contributions obtained in the three approaches are very close. The signs of the penguin contributions are different, and the magnitude in PQCD is larger than those in FA and BBNS:

$$|P_{\rm PQCD}| \sim 5.2 |P_{\rm BBNS}| \,, \quad |P_{\rm PQCD}| \sim 2.7 |P_{\rm FA}| \,. \tag{32}$$

The difference in the total penguin contributions is attributed to the treatment of nonfactorizable and annihilation duagrams. We emphasize that the BBNS results depend on the parameters for factorizable contributions (the transition form factors) and the parameters for nonfactorizable contributions (the meson wave funcitons). Therefore, it is possible to reverse the sign and to increase the magnitude of the penguin contribution by varying these parameters. The penguin contribution in the BBNS approach is smallest because of the cancellation between F^P and M^P. If expressing the amplitudes of the $B_d^0 \to \pi^+\pi^-$ decay as

$$\mathcal{A} = V_t^* |P| e^{i\delta} - V_u^* |T| , \tag{33}$$

with P and T given in Eq. (31), the strong phases δ are about

$$\delta_{\rm PQCD} \sim 123^o \,, \quad \delta_{\rm BBNS} \sim -50^o \,, \quad \delta_{\rm FA} \sim -113^o \,. \tag{34}$$

The predictions for the CP asymmetry of the $B_d^0 \to \pi^\pm\pi^\mp$ decays are presented in Fig. 5. Because of Eq. (32), the CP asymmetry in PQCD is larger than that ($\sim 10\%$ at most) in FA and much larger than that ($\sim 4\%$ at

most) in BBNS. Because of Eq. (34), the sign of the CP asymmetry in PQCD is opposite to those in FA and BBNS. If the B meson wave function in [27] with $\omega_B = 0.4$ GeV is adopted, M^P and also $|P_{\rm BBNS}|$ will increase accordingly, such that the CP asymmetry in the BBNS approach becomes a bit larger. We shall leave the resolution of the above discrepancies to future measurements of CP asymmetries. That is, experimental data of CP asymmetries will provide an appropriate test of the three approaches. Note that all the three approaches give the similar branching ratio $B(B_d^0 \to \pi^\pm\pi^\mp) \sim 4.6 \times 10^{-6}$, which is consistent with the CLEO data [23].

As argued in Sec. III, to account for the $B \to K\pi$ and $\pi\pi$ data simulataneously using the unitarity angle $\phi_3 = 90^o$, the ratio of the penguin contribution to the tree contribution must be as large as 0.1. It is easy to find

$$|P_{\rm PQCD}|/|T_{\rm PQCD}| = 0.12\ , \quad |P_{\rm BBNS}|/|T_{\rm BBNS}| = 0.02\ , \quad |P_{\rm FA}|/|T_{\rm FA}| = 0.04\ , \tag{35}$$

from Eq. (31). Due to the smaller ratio in the BBNS and FA approaches, a larger angle $\phi_3 > 90^o$ must be adopted in order to explain the $B \to \pi\pi$ data [6,24]. As a consequence of the penguin enhancement, the CP asymmetry is also large in the PQCD approach.

VI. SUMMARY

We summarize the comparision among the FA, BBNS, and PQCD approaches as follows:

1. The scale independence of predictions in the FA and BBNS approaches is achieved by the generalized FA method: a μ-dependent evolution factor is extracted from hadronic matrix elements by considering the mixing of the effective operators at a scale below μ. This evolution factor is then combined with the μ-dependent Wilson coefficient to form a scale-independent effective Wilson coefficient. However, the infrared-cutoff and gauge dependences appear. In the PQCD approach the scale independence is made explicit by extending the Wilson evolution down to the hard scale t directly, which is then followed by the second-stage RG evolution evaluated based on six-quark amplitudes. Since external quarks are on-shell, the gauge invariance of PQCD predictions is guaranteed. The infrared-cutoff dependence, treated as a factorization scheme dependence, is removed by the universality of wave functons.

2. Factorizable contributions (hadronic transition form factors) are not claculable in the FA and BBNS approaches, but calculable in the PQCD approach. The inclusion of parton transverse momenta smear the end-point singularity, and Sudakov suppression guarantees that almost all contributions come from the region with $\alpha_s/\pi < 0.3$.

3. Dynamical penguin enhancement exists in the PQCD approach, but not in the FA and BBNS approaches. This enhancement, arising from different evolution effects in the form factors associated with the Wilson coefficient a_1, a_4 and a_6, is cruical for the simultaneous explanation of the $B \to K\pi$ and $\pi\pi$ data using a smaller unitarity angle $\phi_3 \sim 90^o$ [4].

4. Nonfactorizable amplitudes are neglected in the FA approach, but calculable in the BBNS and PQCD approaches. However, without Sudakov suppression, higher-order corrections are not under control in the BBNS approach. The end-point singularity needs to be smeared by taking into account parton transverse momenta and Sudakov suppression. On the other hand, nonfactorizable amplitudes are real in the BBNS approach, but complex in the PQCD approach. The conclusion is the same: nonfactorizable contributions are destructive relative to the penguin contributions and negligible for the evaluation of branching ratios.

5. Annihilation contributions are neglected in the FA and BBNS approaches, but calculable in the PQCD appraoch. The helicity suppression applies only to amplitudes associated with O_4, but not to those associated with O_6. It is found that the O_6 contribution is of the same order as the penguin contribution, and gives a large imaginary part.

6. Strong phases come from the BSS mechanism and the extraction of the μ dependence from hadronic matrix elements in the FA and BBNS approaches, but from annihilation diagrams in the PQCD approach. It has been argued that the two sources of strong phases in the FA and BBNS approaches are in fact strongly suppressed by the charm mass threshold and by the end-point behavior of meson wave functions.

7. Because of the large penguin and annihilation contributions in the PQCD approach, the predicted CP asymmetry in the $B_d^0 \to \pi^\pm\pi^\mp$ decays dominates over those in the FA and BBNS approaches as shown in Fig. 5. Future measurements of CP asymmetries can distinguish the FA, BBNS, and PQCD approaches.

Acknowledgment

We thank M. Bando, Y. Sumino and M. Yamaguchi for organizing the Summer Institute 99 at Yamanashi, Japan, whose active atmosphere stimulated this work, H.Y. Cheng, T. Mannel and A.I. Sanda for helpful discussions, and M. Kobayashi for his encouragement. The works of HNL and YYK were supported in part by the National Science Council of R.O.C. under the Grant Nos. NSC-89-2112-M-006-004 and NSC-89-2811-M-001-0053, respectively, and in part by the Monbusho visiting fellowship from the Ministry of Education, Science and Culture of Japan.

[1] M. Bauer, B. Stech, M. Wirbel, Z. Phys. C **34**, 103 (1987); Z. Phys. C **29**, 637 (1985).

[2] C.H. Chang and H-n. Li, Phys. Rev. D **55**, 5577 (1997).

[3] T.W. Yeh and H-n. Li, Phys. Rev. D **56**, 1615 (1997).

[4] Y.Y. Keum, H-n. Li and A.I. Sanda, hep-ph/0004004; hep-ph/0004173.

[5] M. Beneke, G. Buchalla, M. Neubert, and C.T. Sachrajda, Phys. Rev. Lett. **83**, 1914 (1999).

[6] D.-S. Du, D.-S. Yang and G-H. Zhu, hepph/0005006.

[7] G. Buchalla, A.J. Buras and M.E. Lautenbacher, Review of Modern Physics **68**, 1125 (1996).

[8] A.J. Buras and L. Silvestrini, Nucl. Phys. **B 548**, 293 (1999).

[9] A. Ali and C. Greub, Phys. Rev. D **57**, 2996 (1998).

[10] H.Y. Cheng and B. Tseng, Phys. Rev. D **58**, 094005 (1998).

[11] H-n. Li, Phys. Rev. D **52**, 3958 (1995).

[12] H-n. Li and H.L. Yu, Phys. Rev. Lett. **74**, 4388 (1995); Phys. Lett. B **353**, 301 (1995); Phys. Rev. D **53**, 2480 (1996).

[13] H-n. Li and G.L. Lin, Phys. Rev. D**60**, 054001 (1999).

[14] H-n. Li and B. Melic, Eur. Phys. J. C**11**, 695 (1999).

[15] B. Melic, Phys. Rev. D **59**, 074005 (1999).

[16] C.D. Lu, K. Ukai and M.Z. Yang, hep-ph/0004213.

[17] H.Y. Cheng, H-n. Li, and K.C. Yang, Phys. Rev. D **60**, (1999).

[18] B. Melic, B. Nizic and K. Passek, hep-ph/9802204.

[19] J.C. Collins and D.E. Soper, Nucl. Phys. **B193**, 381 (1981).

[20] J. Botts and G. Sterman, Nucl. Phys. **B325**, 62 (1989).

[21] H-n. Li and G. Sterman Nucl. Phys. **B381**, 129 (1992).

[22] R. Jacob and P. Kroll, Phys. Lett. B**315**, 463 (1993); Erratum-ibid B**319**, 545 (1993).

[23] CLEO Coll., D. Cronin-Hennessy et al., hep-ex/0001010.

[24] W.S. Hou, J.G. Smith, and F. Würthwein, hep-ph/9910014.

[25] H.Y. Cheng, (hepph/9912372), Talk at 3rd Intrnational Conference on B physics and CP violation (BCONF99), Taipei, Taiwan, 3-7 Dec. 1999.; H.Y. Cheng and K.C. Yang, hep-ph/9910291.

[26] N. Isgur and C.H. Llewellyn-Smith, Nucl. Phys. **B317** 526 (1989).

[27] M. Bauer and M. Wirbel, Z. Phys. C **42**, 671 (1989).

[28] C.H. Chen and H-n. Li, in preparation.

[29] Y.H. Chen, H.Y. Cheng, B.Tseng and K.C. Yang, Phys. Rev. D **60** 094014 (1999).

[30] G. P. Lepage and S. J. Brodsky, Phys. Lett. B **87**, 359 (1979); Phys.Rev. D **22** 2157 (1980).

[31] M Bander, D. Silverman and A. Soni, Phys. Rev. Lett. **43**, 242 (1979).

Figure Captions

1. Fig. 1: One of the lowest-order factorizable diagrams for the $B_d^0 \to \pi^+\pi^-$ decay.

2. Fig. 2: Lowest-order nonfactorizable diagrams for the $B_d^0 \to \pi^+\pi^-$ decay.

3. Fig. 3: Lowest-order hard amplitudes for the $B_d^0 \to \pi^+\pi^-$ decay.

4. Fig. 4: Diagrams that give strong phases in the FA and BBNS approaches.

5. Fig. 5: Direct CP asymmetries in the $B_d^0 \to \pi^\pm\pi^\mp$ decays.

Amplitudes	Left-handed column		Right-handed column		PQCD	BBNS
$Re(f_\pi F^T)$	(a)	$4.39 \cdot 10^{-2}$	(b)	$2.95 \cdot 10^{-2}$	$7.34 \cdot 10^{-2}$	$7.57 \cdot 10^{-2}$
$Im(f_\pi F^T)$		–		–	–	$1.13 \cdot 10^{-3}$
$Re(f_\pi F^P)$	(a)	$-3.54 \cdot 10^{-3}$	(b)	$-2.33 \cdot 10^{-3}$	$-5.87 \cdot 10^{-3}$	$-3.04 \cdot 10^{-3}$
$Im(f_\pi F^P)$		–		–	–	$-1.27 \cdot 10^{-3}$
$Re(f_B F_a^P)$	(e)	$5.05 \cdot 10^{-4}$	(f)	$-1.94 \cdot 10^{-3}$	$-1.42 \cdot 10^{-3}$	–
$Im(f_B F_a^P)$	(e)	$2.19 \cdot 10^{-3}$	(f)	$3.72 \cdot 10^{-3}$	$5.91 \cdot 10^{-3}$	–
$Re(M^T)$	(c)	$5.02 \cdot 10^{-3}$	(d)	$-6.55 \cdot 10^{-3}$	$-1.53 \cdot 10^{-3}$	$-7.71 \cdot 10^{-4}$
$Im(M^T)$	(c)	$-3.83 \cdot 10^{-3}$	(d)	$7.03 \cdot 10^{-3}$	$3.20 \cdot 10^{-3}$	–
$Re(M^P)$	(c)	$-2.29 \cdot 10^{-4}$	(d)	$2.75 \cdot 10^{-4}$	$4.66 \cdot 10^{-5}$	$4.17 \cdot 10^{-3}$
$Im(M^P)$	(c)	$1.95 \cdot 10^{-4}$	(d)	$-3.08 \cdot 10^{-4}$	$-1.13 \cdot 10^{-3}$	–
$Re(M_a^P)$	(g)	$1.14 \cdot 10^{-5}$	(h)	$-1.48 \cdot 10^{-4}$	$-1.37 \cdot 10^{-4}$	–
$Im(M_a^P)$	(g)	$-9.12 \cdot 10^{-6}$	(h)	$-1.27 \cdot 10^{-4}$	$-1.36 \cdot 10^{-4}$	–

TABLE I. Amplitudes for the $B_d^0 \to \pi^+\pi^-$ decay from Fig. 3, where F (M) denotes factorizable (nonfactorizable) contributions, P (T) denotes the penguin (tree) contributions, and a denotes the annihilation contributions. Here we adopted $\phi_3 = 90^0$, $R_b = 0.38$, and $\alpha_s(m_b) = 0.2552$ in the numerical analysis for the BBNS approach.

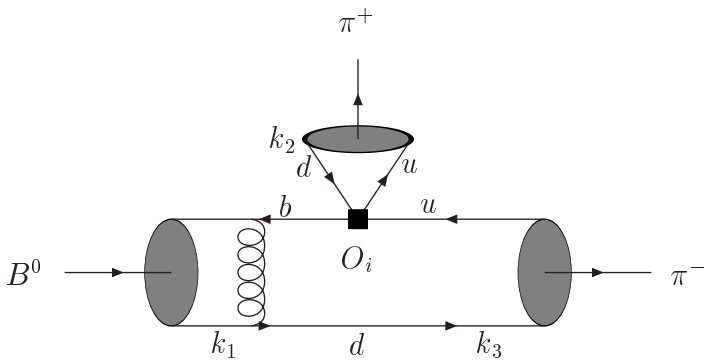

Figure 1

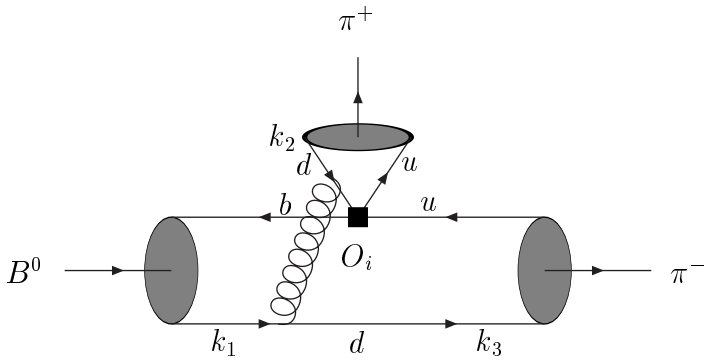

(**a**)

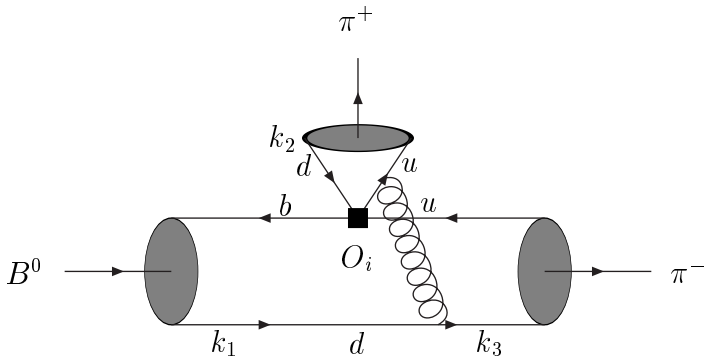

(**b**)

Figure 2

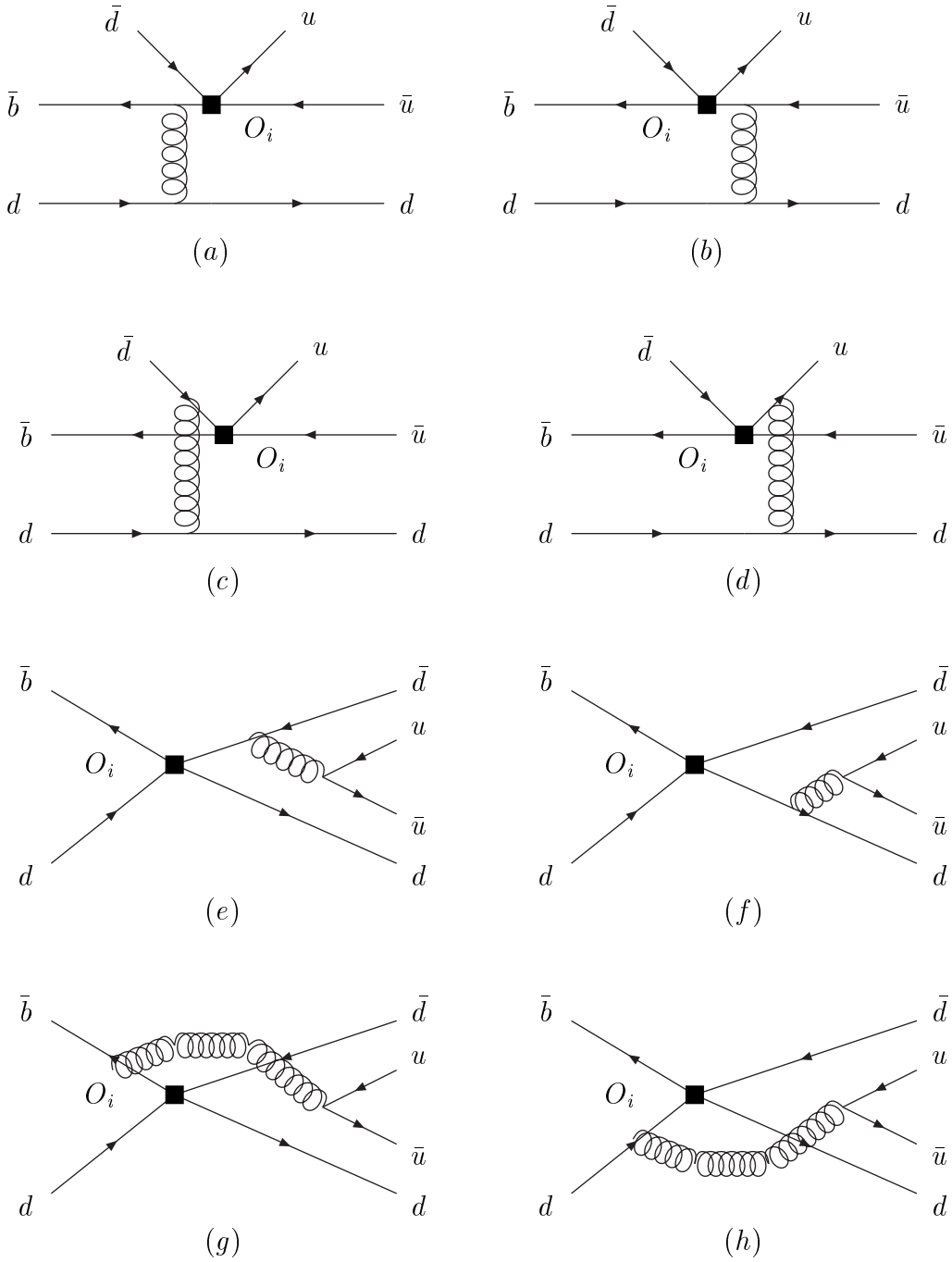

Figure 3

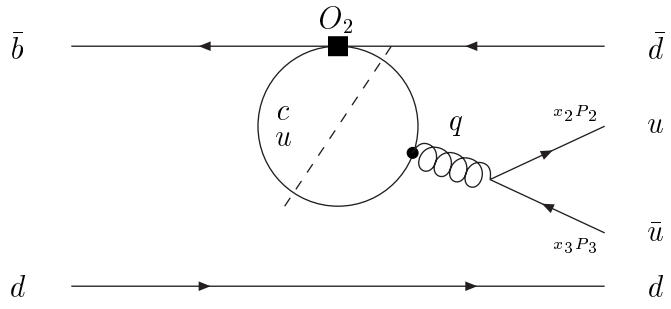
O_2
$\bar{b}$
$\bar{d}$
c
u
q
x_2P_2
u
$\bar{u}$
x_3P_3
d
d

(a)

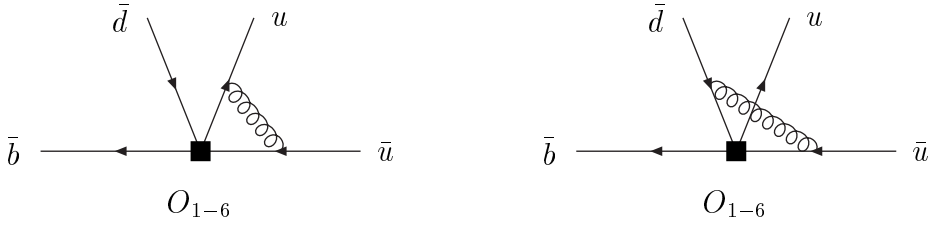
$\bar{d}$
u
$\bar{b}$
$\bar{u}$
O_{1-6}
$\bar{d}$
u
$\bar{b}$
$\bar{u}$
O_{1-6}

(b)

Figure 4

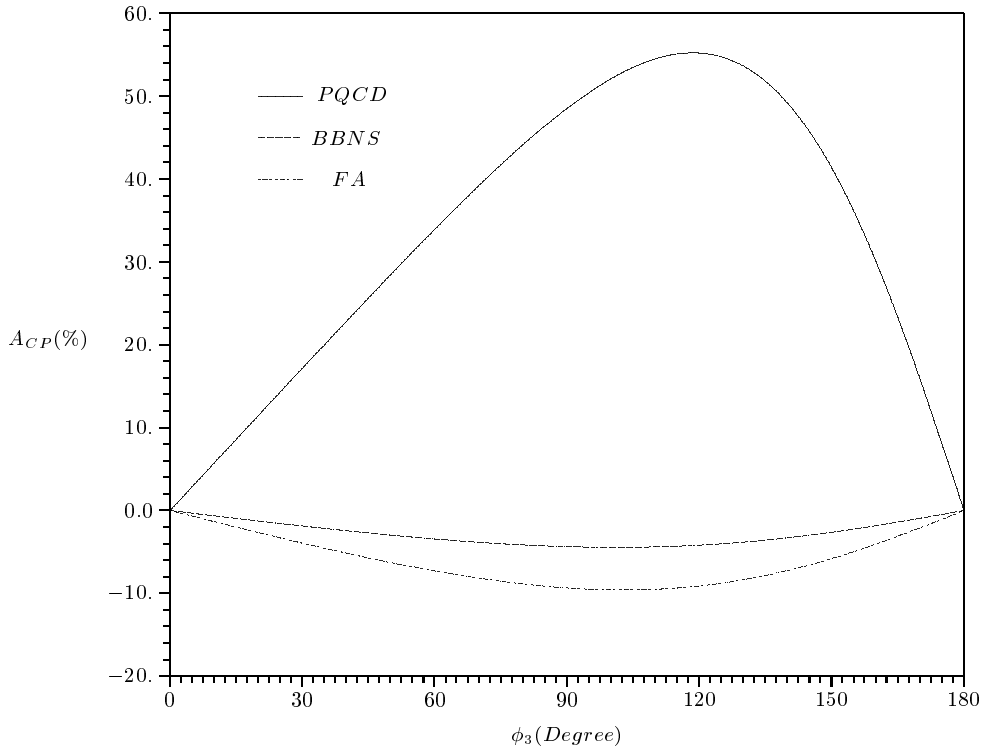
60.
50.
40.
30.
20.
10.
0.0
−10.
−20.
$A_{CP}(\%)$
$PQCD$
$BBNS$
FA
0
30
60
90
120
150
180
$\phi_3(Degree)$

Figure 5